Abnormal grain growth and texture evolution in 99.99% high purity aluminum foil during high and low speed annealing

YUNLEI WANG[a], GUANGJIE HUANG[a,*], XIONG LI[a], QING LIU[a,b]
[a]*College of Materials Science and Engineering, Chongqing University, Chongqing 400044, China*
[b]*National Engineering Research Centre for Magnesium Alloys, Chongqing University, Chongqing 400044, China*

Investigating recrystallization (RX) and abnormal grain growth (AGG) in high purity aluminum foil during the different heating up rates of annealing, it generally analysed the evolution of microstructure and texture. Some of the assumptions discuss the mechanism of individual grain growth abnormal behavior involved the importance of oriented grain distribution and texture component development. According to the experimental data, It showed that the (001) plane texture oriented grain and cube texture {001}<100> are prior to nucleate and grow advantage than other oriented grains. The abnormal grain growth may be controlled by surface energy effect during the high speed annealing (HA) process and final mean grain size far surpass the 110μm of specimen thickness, which is the mainly driving force for grain growth after RX. However, the final average grain size is 64.3μm during the low speed annealing (LA) process and the abnormal grain growth behavior does not occur in this foil.

(Received December 1, 2014; accepted May 7, 2015)

Keywords: Recrystallization, AGG, Texture evolution, Aluminum foil

1. Introduction

Early work on abnormal grain growth (AGG) in crystalline material has received considerable attention followed by to some important aspects. Detailed theories and modeling explanation have been given that, for instance, the theory of a growth equation including normal and abnormal grains in single-phase materials was proposed and defect-model was used to predict the limitation of grain size obtained by Hillert [1]. The effect of impurities and slight deformation as factors modifying the kinetics of normal grain growth after primary RX and further secondary grain growth (abnormal grain growth) in pure iron was investigated by Antonione *et al.* [2]. Monte Carlo (MC) computer simulation method has been used to investigate the abnormal grain growth in a two dimensional matrix under two conditions following curvature to provide driving force solely and difference in the gas-metal surface energy between grains of different crystallographic orientation providing driving force, as revealed by Srolovitz *et al.* [3]. Thompson and co-workers [4] compared the relative rate of secondary (AGG) and normal grain growth with the situation of uniform grain boundary energy which was the only factor affecting boundary motion. Recently, Grest and Anderson *et al.* [5] have investigated the effect of grain boundary mobility anisotropy on AGG for the more realistic cases of grain growth in three dimensions. Based on the theories of Hillert and Thompson [1, 4], Rios [6] has proved the tendency for an abnormal grain to grow depending on the distribution shape in purity materials, which is a complex process. Of course, it considers abnormal grain growth (AGG) and normal grain growth (NGG) as competitive rather than separate processes, this aspect about it has been extensively investigated by a number of authors [1-17] in the past few years.

A number of authors [1-19] have given the investigations of abnormal grain growth in crystalline materials containing aluminum or its alloys. However, it is a little detailed theoretical explanation about abnormal grain growth in high purity aluminum foil during different heating rate in annealing process. So the aim of this paper is to investigate and discuss the mechanism of abnormal grain growth in high purity aluminum foil during different heating up rates of annealing (HA and LA), and also observe the texture evolution during the two different annealing processes.

2. Experimental procedures

Experimental material is 99.99% Al sheet. The impurities present in this material are given in Table.1, thickness of aluminum sheet is cold-rolled from 7.00mm to 0.11mm (110μm) (accumulative reduction is 98%) by a double-roller-mill with multi-passes and then giving two

kinds of annealing heat treatment: (a) High heating (HA) speed (isothermal heat treatment) i.e. put samples into annealing furnace when temperature is 500℃, then take out quickly and water cooling them after holding time is several seconds respectively. (b) Low heating (LA) speed (Non-isothermal heat treatment [20]) via the specimens together with furnace heating up to 180℃and holding time is 1h, then heating up to 500℃ and also holding time is 1h (heating up rate is about 180℃ per hour), it is also water cooled, and many temperature points can be set up from 180℃ to 500℃.

The time-temperature curves are plotted and shown in Fig. 1. The purpose of the different annealing treatment was to activate the different physical mechanism in investigated material. HA and LA, is high and low speed annealing respectively.

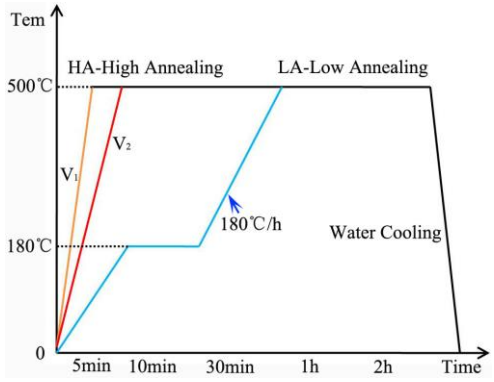

Fig. 1. Temperature-time curves for two different annealing treatment (HA and LA) of investigated material of high purity Aluminum foils.

3. Experimental results

3.1. Microstructure

The deformed samples after annealed at 500℃ for a series of holding time, followed by electro-polishing and anode making-film, observed by Axiovert 40 MAT optical microscope and showing the polarization micrograph of high speed annealing for Fig. 2. And obtained the recrystallized grain evolving from deformed grain to equiaxed grains, for Fig. 2 (a) the average grain size is small, approximately equaling to 96.6μm by compute and distribute relative uniformly. With the annealing time increasing to 400s, Fig. 2(a) the grains grow rapidly and their sizes become larger, the individual grain anomalous grow, that is to say the possess size advantage [21] over others, especially individual grain size larger to their neighboring grains at the annealing time is 800 seconds in Fig. 2(c). The tendency of grain growth is that grain via consuming others to advantage its growth. The annealing time is continuous increasing approximately 3800 seconds. The grain size tends to be stable.

Focus on Fig. 2(d), the micrograph of fully recrystallized after annealed at 320℃, all grains grow normally and their size uniformly distribution in current studying crystallographic spatial, without the abnormal behavior of grain growth. This annealing process is so-called Non-isothermal heat treatment proposed by Schäfer [20], used for the low heating rates of annealing process especially. The grains closely contact with each other and the value of their sizes are similarly. The Another information was given that different colors represented different oriented grains, that is to say the same oriented grains closely contact with other grains, and grain boundary always is not always show within neighboring grains due to the low angle grain boundary insensitivity to polarization light.

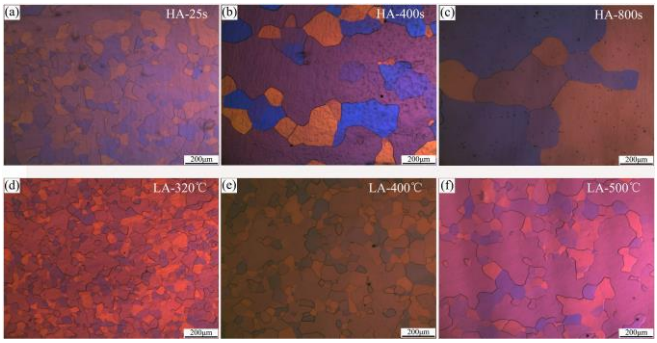

Fig. 2. Polarized optical microscopy map of two different annealing for (a) HA-25s, (b) HA-400s, (c) HA-860s; (d) LA-320 ℃, (e) LA-400 ℃, (f) LA-500 ℃.

3.2. Grain size measurement

The statistical analysis of abnormal grain growth behaviors based on the observation of optical microscope (shown in Fig. 2). A series of experimental data for HA and LA process were obtained via optical microstructure (OM), after using special software to deal with the data of investigated microstructure of specimens and the calculated mean grain sizes for that were plotted for Fig. 3, and showing the distribution of mean grain size.

Compare the high speed annealing with low speed annealing process to observe the tendency of mean grain size distribution (GSD) in for Fig. 3(a) and (b), respectively. On the one hand, there is a significant difference between high speed annealing (iosthermal heat treatment) and low speed annealing (Non-iosthermal heat treatment) for the aspect of grain size, the grain size of high speed annealing is larger and grows abnormally, the diameter of mean grain size is beyond the thickness (110μm) along the normal direction (ND) of investigated sample, which is accompanied with the characteristic of a thin Al film for this aluminum foil, the similar investigation of in-situ observation of AGG in thin Cu films was controled by Sonnweber-Ribic [22]. On the other hand, the grain size of low speed annealing is at a

range of 17.7μm to 64.3μm, without so called catastrophic growing [23], which contacts with their neighboring grains closely to each other, and also its spatial distribution is homogeneous.

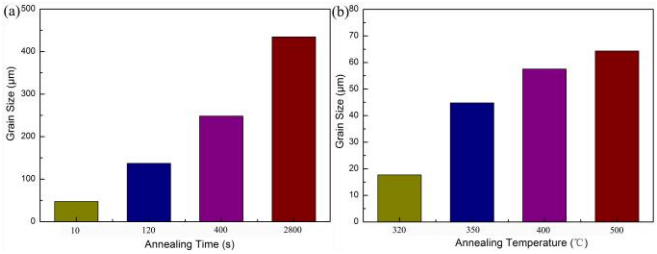

Fig. 3. Mean grian size distribution of (a) HA and (b) LA process.

3.3. Oriented-grain component

Grain growth is accompanied with a change of grain orientation distribution, therefore in turn, the difference of grain orientations impel to grain growth isotropy or anisotropy in the three-dimensional (3D) crystallographic structure. As following the Fig.4, which is exhibiting the orientation image microscopy (OIM) in the high speed annealing process (HA), the measurements were obtained by electron backscatter diffraction (EBSD) equiped with FEI Nova 400 FEG-SEM. The microstructure develops from deformed matrix to recrystallized grain in local RX for Fig. 4(a) at the HA-10s, some individual grains began to nucleate surrounded by deformed matrix, in this situation the stage of recovery is already completed, and accompanied with releasing of deformation storage energy. The serious defect locations act as nucleation sites, local RX preferentially surround the deformed matrix. While the annealing time increasing at 30s (HA-30s), RX is already completed and equiaxed-grain inhomogeneously distributes at the TD-RD plane, the (001) plane-texture grain nuclei starts to grow quickly and anomalously for the red color grain, overrunning the (111) oriented grain in size marked blue color. For the Fig. 4(c) HA-40s, the (101) plane-texture oriented grain grows abnormally and distributes at the crystallographic spatial continuously, which is like a shape of isolated island, its tendency is likely to consume the (001) and (111) plane-texture grains, however it is beyond expectation of that, turning to Fig. 4(d) HA-60s the (001) plane-texture grain contacts with each other and exhibits LAGBs between the same oriented grains, their neighboring oriented grains distribute uniformly around (001) plane-texture grain, this observed the (001) plane-texture grain growth anomalously and occurred predominantly at the crystallographic spatial. The next, the grain growth tendency and relationship of orientation between adjacent grains for this information can be followed by Fig. 6.

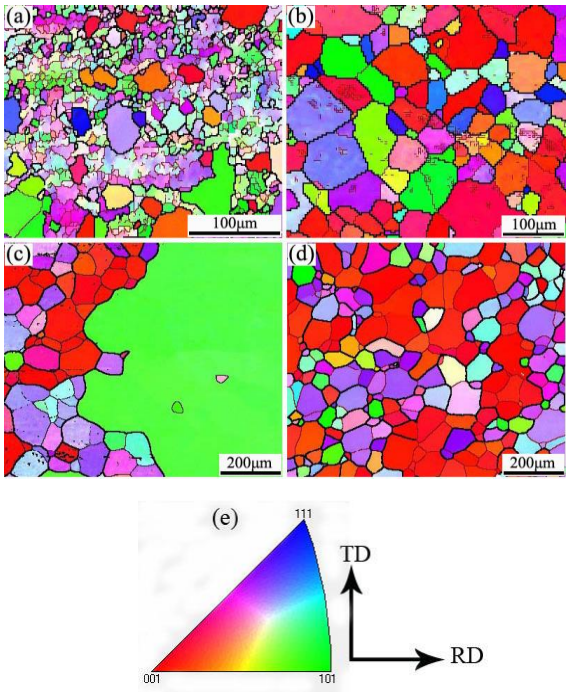

Fig. 4. Orientation image microscope(OIM) of high speed annealing for for (a) HA-10s; (b) HA-30s; (c) HA-40s; (d) HA-60s; (e) Orientation color coded map.

The misorientation angle distribution of high speed annealing is obtained from data processing of electron backscatter diffraction, the first glance to observe that misorientation angle distribute at the range of 2～15° mostly, belongs to low angle grain boundary (LAGB). For Fig. 6(a) the misorientation angle is mainly distributed below 15°, some others distributing at 20～60° was so-called high angle grain boundary (HAGB), and this concept was defined by Lim [24]. With the annealing holding time increasing, the misorientation angle distribution is mostly close to 20～60°, that is to say, which exhibits more HAGBs and grain grows very rapidly, combining with Fig. 6(a) EBSD map of HA-30s. For Fig. 6(a) the misorientation angle distribution tended to 2～10°, which accounts for phenomenon that the neighboring grain boundary is LAGB, and the volume fraction of this LAGB is higher than former. According to the analytical misorientation angle distribution state and deriving the relationship between low angle interfacial energy and misorientation angle from Read and Shockley [25], as that Eq. (1):

$$\gamma_B = \frac{Gb}{4\pi(1-\gamma_0)}\theta(B-\ln\theta) \tag{1}$$

Where γ_B is grain interfacial energy, G is shear modulus, b is dislocation burgers vector, θ is misorientation angle, B is integration constant and depend on atomic mis-arrange energy of dislocation center, is also a constant and depend on G, b of investigated

material. For the Eq.(4) demonstrated the value of γ_B incresed with increment value of θ . However, the high angle interfacial energy has nothing to do with θ and the value is a constant for 0.25～1.0J/m^2, much larger more than low angle interfacial energy. For HA-60s the misorientation angle distribution is as normal distribution clustering within 2～15°and 20～60°, this observed result shows both existing LAGBs and HAGBs, and indicats that LAGBs oriented grains continuously increased their misorientation angle to impel grain to grow rapidly, while HAGBs oriented grains was reduced to total interfacial energy and act as driving force for subsequent grain growth, as a performance of abnormal grain growth for red color region oriented grains of Fig. 4. i.e. the (001) oriented grain grows quickly.

The high purity aluminum sheet was subjected to severe cold deformation and contained high stored energy that is the driving force for subsequent nucleation. The sample is very thin and can be heated through to the definite temperature needed quickly. Therefore, the nucleation can be finished quickly with a lower consumption of stored energy. So the high fraction of stored energy is left after recrystallization, which will effectively stimulate the fast growth of grain size. When the grain size of sample nearly reaches the thickness of the foil, the planes of surface are different due to the different orientations of grains. The different planes of surface will result in great difference in surface energy and maybe facilities to control the abnormal grain growth after RX.

Combining with Fig. 4 of the EBSD map, the all process of Fig. 6 demonstrated that the process undergoing local RX and deformed zone to fully RX in spite of being present most LAGBs to HAGBs, and some oriented grains grow abnormally. So the best explanation of this result is that the neighboring grain absorb each other to reduce total grain boundary interfacial energy being the driving force for grain growth. The low angle subgrain increasing misorientation continuously to transform into high angle grain boundaries. This grain boundary migration induce grain growth. So finally the grain sizes grows lager and reaches the definite size.

The relationship between grain boundary misorientation and grain growth has been investigated [21, 26-28], the grain growth is dependent on sub-grain or grain boundary migration, the grain boundary motion direction for enlarged grain size and growth rate is increasing, in a certain extent, most of the grain do not grow and the size achieves the limitation. Only a few grains grow continuously, it is called abnormal grain growth，this abnormal growth behavior can induce texture component changed and control the final grain orientation.

After analyzing the grain orientation distribution of HA process by IPF color map, the next significant information of LA process is controlled via texture component exhibited for Fig. 5. To get full consideration of oriented grain map, the cubic oriented grain {001}<100> prior to nucleation and predominantly possess distribution full of crystallographic spatial. Focus on Fig. 5(a) LA-180℃ with holding time 1h, the large area deformed matrix is full of S-{123}<634> oriented texture component, and mixed up with the weak cube-{001}<100>, Brass-{011}<211> and Copper-{112}<111> texture component. After recovery, the cube-{001}<100> oriented grains are beginning to nucleation at the high distortion and dislocation density zone in local RX area surrounded by deformed matrix, the high distortion area stores high deformed energy to prepare requirement of energy for nucleation in Fig.5(a) , the red granular grain within black area become nucleation site. When the annealing temperature reaches to 320℃, the microstructure varied from deformed grain to RX grain and composed of cubic-{001}<100> texture component, the S-{123}<634> is similar with R-{124}<211> (is a typical RX texture component) and Goss-{011}<100> texture, Copper-{112}<111>, a small fraction T-cube {001}<110>, some others are Non-index texture components for white color grains. When the annealing temperature is increased to 400℃, the cubic oriented grain almost takes the place of all crystallographic spatial and become the main texture component, at the expense of Goss and Copper texture component for the further growing. During 500℃ and holding time is 1h, the cube-{001}<100> oriented grain becomes a leading texture around Copper and S (R-{124}<211>) texture component, the cubic oriented grain boundaries are LAGBs corresponding to misorientation angle distribution for Fig. 6(b). This LA process demonstrated that the cubic oriented grain begins to nucleate taking advantage of other oriented grains in deformed structure, consuming Brass and other texture with next annealing temperature elevated, and finally cube texture component takes the leading place of texture in almost crystallographic spatial.

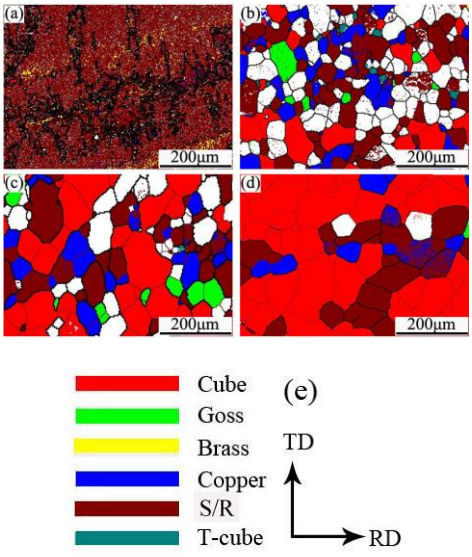

Fig. 5. EBSD mapping of low speed annealing for (a) LA-180℃x1h; (b) LA-320℃; (c) LA-400℃; (d) LA-500℃x1h; (e) Orientation color coded.

Analyse this LA process of misorientation angle distribution corresponding to Fig. 5(a) to (d), the evolution of misorientation angle between neighboring grains reflect the characteristic of grain growth, the LAGBs occur to bring reduction of grain boundary energy and act as a driving force for subsequent grain growth, those grains grow via grain boundary migration and the large grain consumes small grain to impel further grain growth. The HAGBs exist at different orientation neighboring grains, as a result, the special oriented grain possess the growth and size advantage [6], for instance the 40° <111> oriented grain possess the optimal condition for growing in aluminum alloys and grow to a large size, at the expense of other grains, and affect the RX texture components.

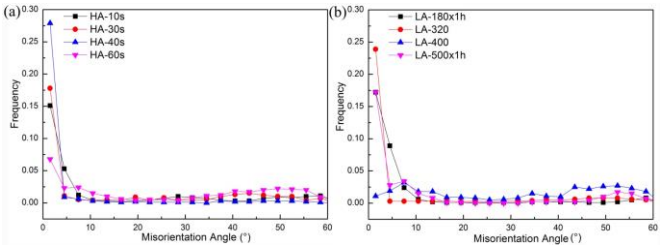

Fig. 6. Misorientation angle of (a) HA process; (b) LA process.

3.4 Texture measurements

The texture measurements of this investigated specimens were carried out by X-ray diffraction using a Rigaku D/MAX 2500 PC X-ray diffractometer. This orientation distribution functions (ODFs) for the deformed and recrystallized specimens were calculated from three complete quarter pole figures (111), (200), and (220), according to the series expansion method. The series were truncated at L_{max}=22 and only terms of an even rank in L were considered. This means some loss in the precision of the final ODFs, but as the actual textures consist of relatively weak and diffuse components, the error in the main components is relatively small.

A. *Texture in the HA Process*

The ODFs of HA process for the sections φ2=45°, 65°, 90° are shown in Fig. 7. The textures in the investigated specimens are almost identical and relatively weak {112}<111> (Copper texture) and strong Cube-{001}<100> texture for the section φ2=45° as the main components, this typical rolling texture is observed in deformed specimens before occuring RX. The next rising annealing holding time at 30s, the copper texture gradually become weakly and disappeared, and transformed it into {001}<100> cube texture component, this volume concentration of cube texture component and its maximum level are plotted in Fig. 7. With the annealing holding time increasing HA-60s the {001}<100> cube texture as the main component distributed in annealing specimens and accompanied with R-{124}<211> texture, this texture components mainly existed in RX specimens and widely observed in high purity Aluminum foils.

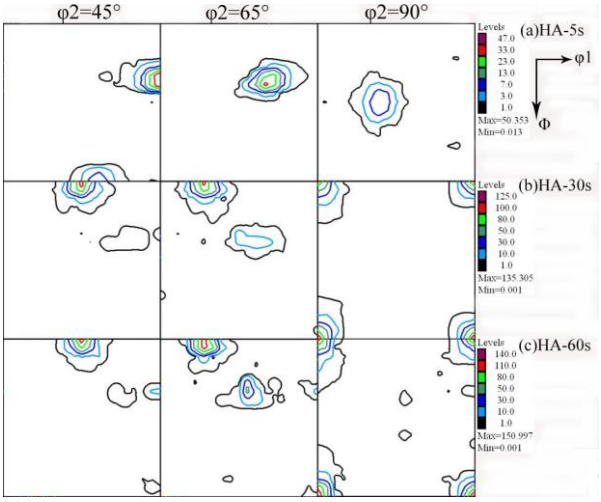

Fig. 7. ODF map of section φ2=45°, 65°, 90° for (a) HA-5s; (b) HA-30s; (c) HA-60s.

B. *Texture in the LA Process*

The corresponding texture measurement of LA process using XRD and shown in Fig. 8. The cold rolled aluminum foil sheet is annealed at 180℃, its initial texture components consist of Copper texture {112}<111> and Brass texture {011}<211> in φ2=45°, it is also a typical rolling texture, the foil undergos recovery state, this low temperature is not enough for RX occurring. With the annealing heating temperature from 180℃ elevated to 350 ℃ and 500 ℃, the {112}<111> Copper and {011}<211> Brass texture component gradually became weak and transformed into cube texture component {001}<100>, finally the Brass-{011}<211> disappeared completely, when the annealing temperature is 500℃, it composed of strong cube {001}<100> texture, it implied that the annealed foil occuring local RX at 350℃ and fully RX at 500℃. All the process in both HA and LA, there are the weak Goss texture {011}<100> and some S texture components {123}<634> (it is similar with R-{124}<211> texture during recrystallized specimens). The volume concentration level value of those texture components for LA process is significantly higher than HA process, the experimental data are shown in Fig. 7 and Fig. 8.

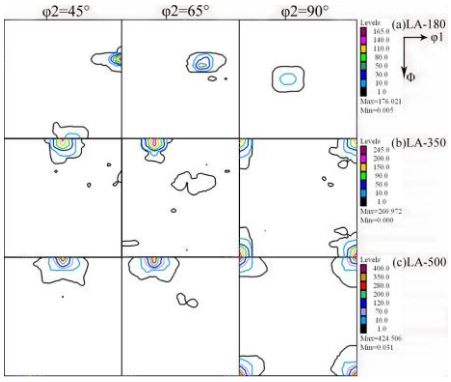

Fig. 8. ODF map of the section φ2=45°, 65°, 90° for (a) LA-180 ℃x1h; (b)LA-350 ℃; (c)LA-500 ℃x1h.

The texture evolution of annealed aluminum foil is contributed to discussing the mechanism of crystall microstructure deformation, the influence of the changing on slip system and dislocation arrangement [29] on stored energy and crystall orientation are significant.

C. *Compare the Texture Volume Fraction of HA with LA Process*

As can be seen that only the fraction of cube texture component {001}<100> increased through HA and LA processes from statistical data of XRD. However the other four mainly texture components decreased with two different annealing processes, this quantitative measurement variation of texture volume fraction for macro-area during HA and LA (i.e. isothermal and Non-isothermal annealing process) is obviously observed. Finally, the cubic oriented grain is predominant RX texture components. The variation tendency of detailed data is plotted in Fig. 9.

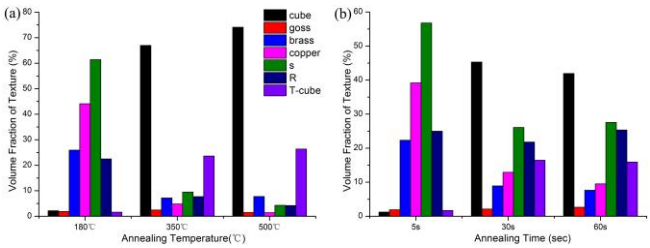

Fig. 9. The texture volume fraction of (a)HA and (b) LA process.

4. Discussion

A. *Grain growth mechanism:*

The investigated specimens of 99.99% high purity aluminum foils volume concentration of impurities is extremely low (following by the Table 1), that is to say the aluminum foil almost dissolve out without any second-phase particles and impurities. Establish one model for grain growing abnormally and based on the following situation and pre-existed theories, the abnormal grain grow behavior need two necessary conditions, as the first one is that the grain size grows to far surpass thickness of aluminum foil along to ND plane at the elevated temperature, the other one is the existence of large size and low surface energy grains. After consisted of these two necessary conditions, the abnormal grain growth may occur.

Table 1. Chemical composition of the investigated aluminum (mass content in ppm).

Al	Si	Fe	Cu	Mn	Mg	Ni	Zn	Ti
Bal.	5-10	8-12	8-35	1-3	15-20	1-3	1-5	1

The inhibition of normal grain growth by texture may lead to the promotion of abnormal grain growth, and a review of the extensive work in this field is given by previous work. Therefore, the effect of texture induce abnormal grain growth in many cases normal grain growth is restricted by a number of factors such as particles and free surfaces in addition to texture, in which case it is difficult to quantify the role of texture in abnormal grain growth. So it established the model in Fig. 10.

Followed by the Fig. 10, the model is explained for controlling grain growth via free surface energy, as assumption that *Ts* is surface tension, T_B is interface line tension along grain boundary, specimen thickness is 110μm, this sections is along the normal direction (ND) and rolling direction (RD), grain *1* is an abnormally grown grain, others are normally grown grains. The grain size grows larger outside along the sample's thickness direction, at this moment the large grain-body is cut off by sample edge, one significant information for grain *1*, the superficial area possess more fraction than grain boundary area obviously. Therefore a new equation expresses the requirement of abnormal grain growth occurring:

$$\sigma_S > \gamma_B \tag{2}$$

$$Ts \geq T_B \sin\theta \tag{3}$$

Where σ_s is surface energy, γ_B is interfacial energy, θ is the cut-off grain intersection angle between surface tension T_B and sample edge, and the details turn to Fig. 10. As is known that grain boundary motion drives grain growth, in this paper the mean grain size is 226.7μm at 500℃ and holding time 400 seconds far surpass the thickness of aluminum foil (110μm), so the classical theory is that surface energy is at the place of

pre-dominant.

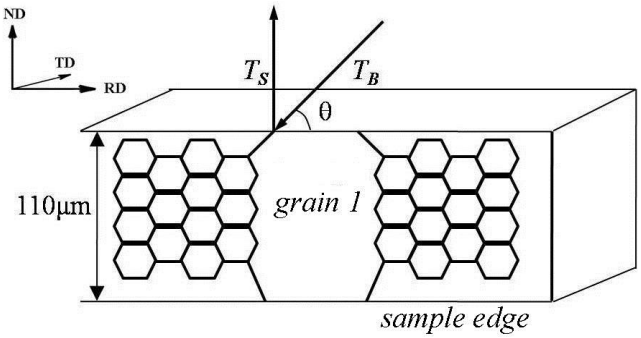

Fig. 10. Schematic diagram of controlling grain growth by free surface energy, Ts is surface tension, T_B is interface line tension along to grain boundary, the specimen thickness is 110μm, this sections along the normal direction (ND) and rolling direction (RD), grain 1 is an individual abnormal growth grain, and others are normal growth grains.

As we know that a grain boundary moves with a velocity in response to the net pressure on boundary (V=MP), when the grain size is far surpass the thickness of aluminum foil along the ND after recrystallization, the surface energy is more than interfacial energy obviously. Therefore, the difference between surface energy and interfacial energy act as a driving force for subsequent grain growth. In Fig. 10, so the T_B is interface line tension along to grain boundary (not parallel to the surface), while the T_S is perpendicular to the foil surface, this model is well enough to illustrate the energy difference acting as a driving force for grain growth.

Therefore the surface energy is a dominant factor to control grain growth, it is so-called surface energy inducing abnormal grain growth, and the driving force provided for grain growth applied by a number of researchers, such as Hillert [1], Huang and Humphreys [30], shown as Eq.(4):

$$\Delta P = \sigma_s - \gamma_B = V/M \tag{4}$$

The present work experimentally confirms grain growth, and the grain growth velocities are found to calculate form Eq.(4), if the net driving force value *ΔP* and known the grain boundary mobility *M* were known. This further detailed research for studying high purity aluminum foils should be continuous and has a long way to go.

B. *Texture evolution*

The (100) and (111) pole figures for 95% cold rolled aluminum earlier were investigated by Grewen and Hubert [31], copper-{112}<111>, brass-{110}<112>, S {123}<634>, those are commonly used to describe the textures.

The texture components of present specimens for HA and LA process has been identified of rolling textures and recrystallized textures, the main focus on the local recrystallized area within deformed matrix, due to the abundant information and key transition point for recrystallized grain nucleation, which contributed to analyzing and discussing the proper mechanism for RX.

Pay attention to the Fig. 11(a) and (c), the texture components are almost the same with each other and can be identified as typical rolling textures although using different annealing treatment, which consist of the brass-{110}<112> texture copper-{112}<111> and S-{123}<634> texture components, the maximum intensity of annealing texture before occurring RX is discrepant and has relationship with recovery closely, after subsequent HA and LA heat treatment the texture component is transformed into a typical annealed RX texture following Fig. 11(b) and (d), existing in experimental high purity aluminum foil. (b) HA-60s mainly contains cube-texture and small fraction copper-texture, however (d) LA-500x1h is almost composed of cube texture, it is implied that the stored energy changed during recovery stage result in residual energy and dislocation arrangement control the RX texture. And the stored energy variation is studied in next paper.

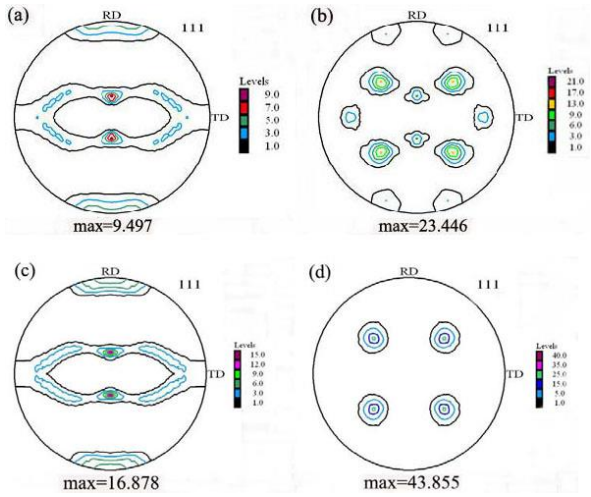

Fig. 11. XRD measured pole figure for (a) HA-5s; (b) HA-60s; (c) LA-180x1h; (d) LA-500x1h.

The (001) plane-texture oriented grain and cube texture component grain may initially grow rapidly to a size sufficient for further growth in subsequent RX and grain growth process. The Goss-{011}<100>, S-{123}<634> and Copper{112}<111> components are under the passive positions, after competing with cube texture, those texture components are very easily absorbed by cubic oriented grain, even gradually disappear in the

crystallographic spatial, so it determines the final RX texture.

5. Summary and conclusions

The textural and microstructural change during this two different annealing, i.e. HA and LA process are undergoing deformed and recrystallized observation of 99.99% high purity aluminum foil. From the obtained work carried out, the following conclusions can be drawn:

1. Observed abnormal grain growth in HA process, the mean grain size is larger and surpasses sample thickness (110μm) along the ND. However, during the LA process without the abnormal behavior for those two aspects, those conclusions go against the typical recrystallization theories.

2. The EBSD map of OIM gives a strong evidence for research on the mechanism of RX nucleation and oriented grain growth. The (001) plane-texture oriented grains prior to grow and surround the other grains, and cubic oriented grain preferentially nucleates in the site of high distortion energy areas.

3. The mean grain growth of its size far exceeds the specimen's thickness, the effect of grain surface energy is greater than that of interfacial energy, so the surface energy is a key factor for grain growth and provides the driving force, however this is just a qualitative analyze for the present research.

Acknowledgments

This study is financially supported by the Chongqing Municipal Programs for Science and Technology (CSTC, 2010AA4047) and National Natural Science Foundation of China (No.50901092).

References

[1] M. Hillert, Acta metallurgica, **13**, 227 (1965).
[2] C. Antonione, G. D. Gatta, G. Riontino, G. Venturello, Journal of Materials Science, **8**, 1 (1973).
[3] D. J. Srolovitz, G. S. Crest, M. P. Anderson, Acta metall, **33**, 2233 (1985).
[4] C. V. Thompson, H. J. Frost, F. Spaepen, Acta metall, **35**, 887 (1987).
[5] G. S. Grest, M. P. Anderson, D. J. Srolovitz, A. D. Rollett, Scripta Metallurgica, **24**, 661 (1990).
[6] P. R. Rios, Acta metall mater., **40**, 2765 (1992).
[7] Andersen, Ø. Grong, Acta metall, mater., **43**, 2673 (1995).
[8] Andersen, Ø. Grong, N. Ryum, Acta metall, mater., **43**, 2689 (1995).
[9] A. D. Rollett, W. W. Mullins, Scripta Materialia, **36**, 975 (1997).
[10] P. R. Rios, Acta mater, **45**, 1785 (1997) -1789.
[11] B. B. Straumal, U. W. Gust, L. Dardinier, J. L. Hoffmann, V. G. Sursaeva, L. S. Shvindlerman, Materials and Design, **18**, 293 (1997).
[12] P. R. Rios, Scripta Materialia, **38**, 1359 (1998).
[13] P. R. Rios, Scripta Materialia, **39**, 1725 (1998).
[14] P. R. Rios, K. Lücke, Scripta mater, **44**, 2471 (2001).
[15] N. M. Hwang, S. B. Lee, D. Y. Kim, Scripta mater, **44**, 1153 (2001).
[16] Y. Estrin, G. Gottstein, E. Rabkin, L. S. Shvindlerman, Acta mater, **49**, 673 (2001).
[17] J. M. Feppon, W. B. Hutchinson, Acta Materialia, **50**, 3293 (2002).
[18] Y. Huang, F. J. Humphreys, Acta mater, **48**, 2017 (2000).
[19] H. P. Kneynsberg, C. A. Verbraak, M. J. T. Bouwhuijs, Materials Science and Engineering, 171 (1985).
[20] C. Schäfer, V. Mohles, G. Gottstein, Acta Materialia, **59**, 6574 (2011).
[21] P. R. Rios, M. E. Glicksman, Acta Materialia, **54**, 5313 (2006).
[22] P. Sonnweber-Ribic, P. A. Gruber, G. Dehm, H. P. Strunk, E. Arzt, Acta Materialia, **60**, 2397 (2012).
[23] O. M. Ivasishin, S. V. Shevchenko, S. L. Semiatin, Scripta Materialia, **50**, 1241 (2004).
[24] A. T. Lim, D. J. Srolovitz, M. Haataja, Acta Materialia, **57**, 5013 (2009) .
[25] W. T. Read, W. Shockley, Physical Review, **78**, 275 (1950).
[26] H. C. Kim, C. G. Kang, M. Y. Huh, O. Engler, Scripta Materialia, **57**, 325 (2007).
[27] F. Liu, R. Kirchheim, Scripta Materialia, **51**, 521 (2004).
[28] S. B. Lee, W. Sigle, M. Rühle, Acta Materialia, **50**, 2151 (2002).
[29] A. Godfrey, Q. Liu, Scripta Materialia, **60**, 1050 (2009).
[30] Y. Huang, F. J. Humphreys, Materials Chemistry and Physics, **132**, 166 (2011).
[31] J. Grewen, J. Huber, Recrystalliztion of Metallic Materials, 111 (1978).

*Corresponding author: gjhcqu@gmail.com